Life-Cycle Seismic Response Analysis of RC Bridges Considering Chloride Induced Corrosion

Chao Li[1, 2], Hong Hao[2], Kaiming Bi[2] & Hongnan Li[1]

1. Corresponding Author. PhD student, Institute of Earthquake Engineering, Dalian University of Technology, Dalian 116024; Department of Civil Engineering, Curtin University, Kent Street, Bentley WA 6102.
   Email: lichao17007@163.com

2. Professor, Department of Civil Engineering, Curtin University, Kent Street, Bentley WA 6102. Email: hong.hao@curtin.edu.au

3. Lecturer, Department of Civil Engineering, Curtin University, Kent Street, Bentley WA 6102. Email: kaiming.bi@curtin.edu.au

4. Professor, Institute of Earthquake Engineering, Dalian University of Technology, Dalian 116024. Email: hnli@dlut.edu.cn

Abstract

This paper studies the seismic responses of corrosion-damaged RC bridges under spatially varying seismic ground motions. The chloride induced corrosion damage to the bridge is considered in the analysis. Based on the time-variant chloride corrosion current density, the extent of the reinforcement corrosion in the bridge piers is estimated. The probability distributions of bridge column reinforcement diameter and yield stress at different time steps after the bridge having been in service are calculated using Monte Carlo simulation method. The uncertainties related to the bridge parameters are considered and the Latin hypercube sampling method is employed to build the probabilistic finite element models of the bridge structure at different time steps along its service life. Spatially varying ground motions at different bridge supports are simulated to be compatible with the response spectra in the Chinese seismic design code and an empirical coherency losses function between each other. Responses of the corroded RC bridge subjected to the simulated spatially varying ground motions are calculated, and the degradation of the seismic performance throughout the service life of the bridge is studied.

Keywords: RC bridges, seismic response, chloride induced corrosion, spatially varying ground motions

1. INTRODUCTION

Bridge structures play a significant role in the development of modern society. Their damage during earthquakes will lead to enormous economic loss. Recently, reports from the American Society of Civil Engineers indicated that more than 20% of the America's bridges need repair or replacement to sustain their normal services and anti-seismic capacities (ASCE 2013). During the life-cycles of reinforced concrete bridges, chloride induced corrosion is one of the main sources that cause structural performance degradation. Neglecting the corrosion effects may lead to significant underestimation of the life-cycle seismic response of

bridges in corrosive environments. In this paper, the seismic response analyses of RC bridges are conducted by considering the chloride induced corrosion effects.

Based on the chloride induced corrosion models of reinforced concrete structures, many researchers have considered the corrosion-induced structural condition deterioration in their studies of the seismic responses of RC bridges during their life-cycles. Simon *et al*. (2010) investigated the effect of corrosion induced reinforcement sectional area reduction and concrete cover spalling on the seismic responses of RC bridges. Alipour *et al*. (2010) performed a life-cycle seismic performance study of RC highway bridges by considering the degradation of column reinforcement diameter and yield strength induced by chloride corrosion. Ghosh *et al*. (2010) carried out a system level time-dependent seismic response analysis by considering the combined influences of RC column and steel bearing corrosions. All these studies indicate that, owing to the process of chloride induced corrosion, the seismic responses of RC bridges increase during their life-cycles.

To better understand the increasing trend of the life-cycle seismic responses of corroded RC bridges, a reasonable chloride induced corrosion model is essential. Many research results (e.g., Liu and Weyers 1996; Vu and Stewart 2000) have shown that the corrosion rate of reinforcement bars in the RC components exposed to the attack of chloride ions decreases with time. However, in most seismic response analyses reported in the literature, a constant corrosion rate is assumed, this might lead to an unreasonable estimation of the lifetime seismic responses of the corroded RC bridges. Moreover, the uniform ground motions are usually used as inputs in the life-cycle seismic response studies of RC bridges. In reality, many research results (e.g., Zanardo *et al*. 2002; Bi and Hao 2013) indicated that the spatially varying ground motions have a great influence on the responses of long span RC bridges.

This paper studies the life-cycle seismic responses of a chloride induced corrosion affected RC bridge. The spatially varying ground motions are stochastically simulated and used as inputs in the analysis. The time-dependent chloride corrosion rate and the uncertainties of structural, material and corrosion parameters are considered in the numerical simulations. The numerical results highlight the importance of considering the chloride induced corrosion and ground motion spatial variability in the seismic response analysis of corroded RC bridges.

2. BRIDGE MODELLING WITH CHLORIDE CORROSION

2.1 Bridge details

A three-span continuous RC bridge designed according to the Chinese design code (JTG/T B02-01 2008) is taken as an example in this study. The bridge is located in a serious chloride corrosion offshore environment. The elevation view and cross sections of the bridge is shown in Figure 1.

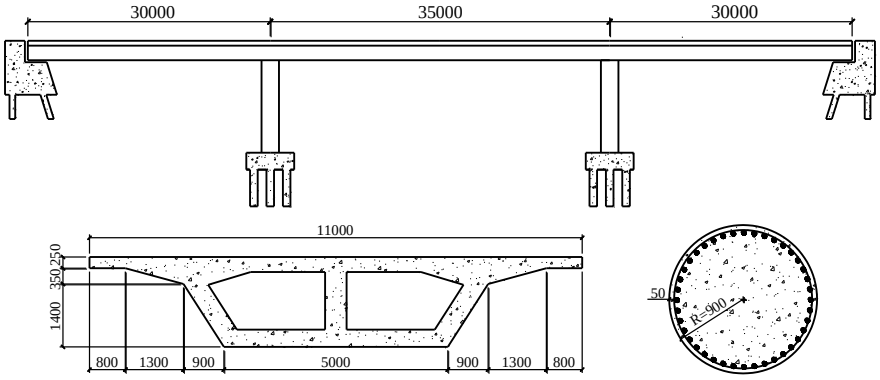

Figure 1. Elevation view and the cross section diagrams of the example bridge (unit: cm, not to scale)

The superstructure is a concrete double-cell box girder with a uniform cross section. The piers are reinforced concrete single columns with a circular section. The water cement ratio of concrete is 0.5 and the reinforcement cover depth is 50 mm. A 50 mm gap is introduced between the superstructure and abutment. Since the piers are the most vulnerable elements during earthquake actions, the chloride induced corrosion is only considered for the piers, the corrosion of the superstructure and the abutments are neglected.

2.2 Chloride induced corrosion

In an offshore environment, the chloride ions are accumulated on the surface of RC bridges under the transportation of sea winds. The diffusion of chloride ions in concrete is initiated due to the chloride concentration difference between the surface and interior part of the concrete. The corrosion initiation time of bridge column reinforcements can be expressed as (Stewart and Rosowsky 1998)

$$T_i = \frac{d_c^{\,2}}{4D_c}\left[\text{erf}^{-1}\left(\frac{C_s - C_{cr}}{C_s}\right)\right]^{-2} \tag{1}$$

where d_c is the depth of the concrete cover; D_c is the coefficient of diffusion; C_s and C_{cr} represent the chloride concentration on the cover surface and the threshold chloride concentration, respectively. In this study, the probability distributions of these parameters are identified in Table 1. Monte Carlo simulation method is adopted to calculate the corrosion initiation time. It is found that the simulation converges when sample size reaches 50000. A lognormal distribution with a mean of 15.4 years and a standard deviation of 8.7 years can be a good fit for the corrosion initiation time of the column reinforcements.

Table 1. Probability distribution models of the parameters related to the reinforcement corrosion initiation time

Parameter	Unit	Distribution	Mean	COV
d_c	mm	Lognormal	50	0.1
C_s	kg/m^3	Lognormal	2.95	0.49
C_{cr}	kg/m^3	Uniform(0.6-1.2)	0.9	0.19
D_c	cm^2/s	Lognormal	3×10^{-8}	0.3

In the reinforcement corrosion stage, the water-insoluble iron hydroxide produced by corrosion will attach to the reinforcement surface and decrease the corrosion rate. In this study, the empirical time-varying chloride current density model prospected by Vu and Stewart (2000) is employed to calculated the corrosion degree of the reinforcements, this model can be expressed as

$$i_{corr}(t_i) = 0.85 i_{corr,0} t_i^{-0.29} \tag{2}$$

$$i_{corr,0} = \frac{37.8(1-w/c)^{-1.64}}{d_c}(\mu\text{A}/\text{cm}^2) \tag{3}$$

in which t_i represents the time after corrosion initiation, $i_{corr,0}$ is the corrosion current density at the corrosion initiation time, w/c is the water to cement ratio and d_c is the concrete cover depth (cm).

Based on experimental results, Du *et al.* (2005) proposed the time-dependent diameter and yield strength of the reinforcements in RC components under chloride induced corrosion:

$$d_s(t_i) = \sqrt{1 - Q_{corr}(t_i)} \cdot d_{s0} \tag{4}$$

$$f_y(t_i) = (1.0 - \beta_y Q_{corr}(t_i))\, f_{y0} \tag{5}$$

where $d_s(t_i)$ and $f_y(t_i)$ are respectively the reinforcement diameter and yield strength at time after corrosion initiation, d_{s0} and f_{y0} are the initial reinforcement diameter and yield strength, respectively, β_y is the strength reduction factor, $Q_{corr}(t_i)$ denotes the percentage of the corroded mass relative to the initial mass of the reinforcement. By considering the time-varying property of the chloride current density, the equation of the percentage of the reinforcement corroded mass relative to the initial mass can be presented based on Vu and Stewart's model (2000):

$$Q_{corr}(t_i) = \frac{4x_{corr}(t_i)}{d_{s0}}\left(1-\frac{x_{corr}(t_i)}{d_{s0}}\right) = \frac{2.10(1-w/c)^{-1.64}}{d_c d_{s0}} t_i^{0.71} - \frac{1.10(1-w/c)^{-3.28}}{d_c^{\,2} d_{s0}^{\,2}} t_i^{1.42} \qquad (6)$$

where x_{corr} is the corroded depth of the reinforcement and equals to $0.0116 i_{corr} t_i$. Combining Equation (6) with (4) and (5), the reinforcement diameter and yield strength at any time of the bridge's life-cycle can be calculated. Considering the uncertainties of the related parameters, the probabilistic distributions of the reinforcement diameter and yield strength are calculated using Monte Carlo simulation, which are shown in Table 2.

Table 2. Means and coefficients of variation (COV) of the column reinforcement diameter and yield strength corresponding to the number of years of the bridge in service

t /year		0	15	30	45	60	75	90
d_s(t)/mm	Mean	40	35.39	32.47	29.95	27.69	25.57	23.55
	COV	0.02	0.0321	0.0478	0.0651	0.0830	0.1048	0.1281
f_y(t)/MPa	Mean	400	374.02	359.08	347.43	337.95	329.48	322.21
	COV	0.08	0.0807	0.0818	0.0826	0.0842	0.0850	0.0857

2.3 Numerical modelling

The OpenSees analysis platform is employed to model the example RC bridge. Since the superstructure is required to remain in linear elastic range in the seismic design of bridges, the superstructure is modelled with elastic beam-column elements, while the columns are modelled with nonlinear beam-column elements. Rigid links are used to connect the superstructure and the pier columns. The abutments are modelled by a rigid element with a length of the superstructure width and a rigid connection is placed between the superstructure centreline and the rigid element. The rigid element is supported by an elastic spring in the vertical direction and nonlinear zero-length elements with a passive stiffness k_a in the two horizontal directions at the two ends (Aviram *et al*. 2008). A gap element is used to model the gap between the superstructure and the abutment.

The parameter uncertainties may have a significant effect on the seismic responses of bridge structures (Pan *et al*. 2007). In this study, the uncertainties in structural, material and chloride induced corrosion related parameters, i.e., the column concrete compressive strength (f_c), the mass per unit length of the deck (m_d), the abutment stiffness (k_a), the expansion gap width (w_g) and the above obtained column reinforcement diameter ($d_s(t_i)$) and yield strength ($f_y(t_i)$), are considered. Latin hypercube sampling method is employed to build 10 3D finite element models at every 15-year time step after the corrosion initiation time.

3. SIMULATION OF SPATIALLY VARYING GROUND MOTIONS

The 3D spatially varying ground motions are stochastically simulated based on the method proposed by Bi and Hao (2013). In the present study, the seismic ground motions at different supports are compatible with the Chinese seismic response spectra. Two site conditions, i.e.: Class I (firm site) and Class II (medium site) are considered. The response spectra for the two sites are shown in Figure 3. The spatial variation of time histories at different supports of the

bridge is modelled by an empirical coherency function proposed by Hao *et al.* (1989), which can be expressed as

$$\gamma_{ij}(i\omega, d_{ij}) = \exp(-\beta d_{ij}) \exp\left[-\alpha(\omega)\sqrt{d_{ij}}(\omega/2\pi)^2\right] \exp(i\omega d_{ij}/v_{app}) \tag{7}$$

in which

$$\alpha(\omega) = \begin{cases} 2\pi a/\omega + b\omega/2\pi + c, & 0.314\,rad/s \le \omega \le 62.83\,rad/s \\ 0.1a + 10b + c, & \omega > 62.83\,rad/s \end{cases} \tag{8}$$

where d_{ij} is the distance between location i and j; a, b, c and β are constants obtained from regression analysis of the ground motions of Event 45 of the SMART1 array located in Taiwan, and these parameters represent highly correlated ground motions.

3D spatially varying ground motions at four bridge supports are simulated independently. The intensity of the vertical component is assumed to be 2/3 times of the horizontal components, whose peak ground acceleration (PGA) are 0.4g. The duration and time interval of the simulated time histories are 20.47 and 0.01s, respectively. In this study, 5 cases of spatially varying ground motions are simulated and they are listed in Table 3. For each case, 120 sets of spatially varying ground motions are simulated, and each set consists of twelve time histories, i.e., two horizontal and one vertical spatial motion at each of the four supports. It should be noted that in the table 'F' stands for firm site condition, 'M' medium site condition; 'Perfectly' and 'Intermediately' represents perfect and intermediate correlation between spatial ground motions. More information regarding ground motion spatial variation and simulation can be found in Hao et al. (1989) and Bi and Hao (2013).

Table 3. Spatially varying ground motion cases

Case	v_{app} (m/s)	Coherency	Site
1	infinite	Perfectly	FFFF
2	500	Perfectly	FFFF
3	infinite	Intermediately	FFFF
4	500	Intermediately	FFFF
5	500	Intermediately	MFFM

Figure 2 plots the horizontal in-plane spatially varying accelerations and displacements for the heterogeneous site (Case 5). It can be noted that the differences between the spatial motions at abutment supports and those at column supports are very evident. This is because the local site effect can further increase the spatial variations of the ground motions. Moreover, the ground motions on the medium site consist of more low frequency contents and possess lager peak ground motion displacements compared with those on the firm site. Figure 3 shows the comparison of response spectra of the simulated ground motions and the prescribed models, good matches can be observed.

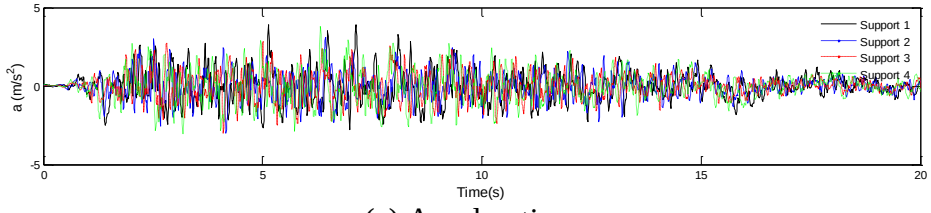

(a) Accelerations

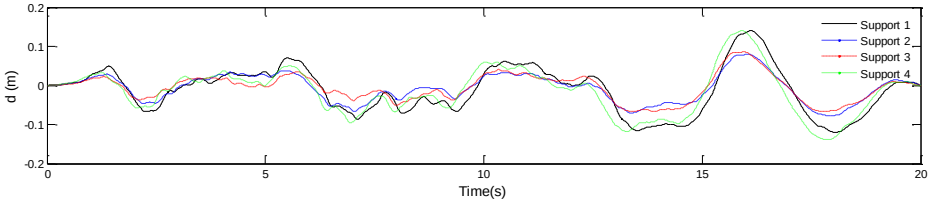

(b) Displacements

Figure 2. Generated spatially varying ground motions on heterogeneous site (Case 5)

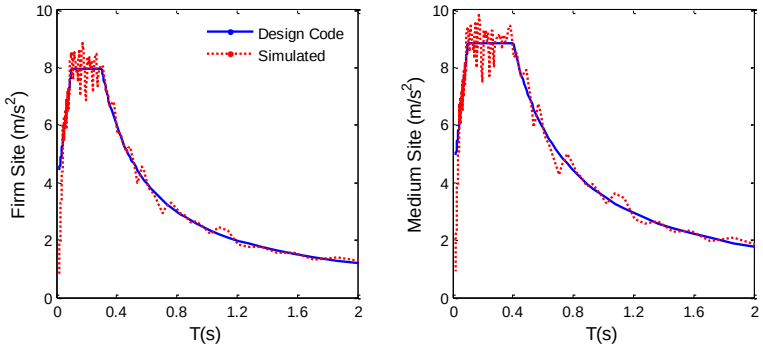

Figure 3. Comparison of the simulated acceleration and the code response spectrum

4. NUMERICAL ANALYSIS

Nonlinear time history analyses are conducted for the example RC bridge models at different time steps under the spatially varying ground motions. As stated above, a total of 10 bridge models are developed at each time step with a 15-year interval after the corrosion initiation time. The simulated 120 sets spatially varying ground motions are equally divided into 10 groups. For bridge models at every time step, the responses of the bridge model subjected to the simulated ground motions are calculated. A total number of 5 (ground motion cases) $\times$7 (time steps) $\times$10 (bridge models) $\times$12 (sets of ground motions) =4200 nonlinear time history analyses are carried out in the present study.

4.1 Modal analysis

Figure 4 plots the fundamental vibration frequencies of the 10 bridge models at each time step during the bridge's service life. The mean frequency at each time step is also calculated. The mean fundamental frequencies of the corroded bridges at initial and 90 years after corrosion initiation are respectively 2.226 and 2.022 Hz, with a decreasing of 9.17%. It can be noted that the degradation speed of the fundamental frequency slows down with time because the chloride induced corrosion current density decreases with time in the bridge's life-cycle.

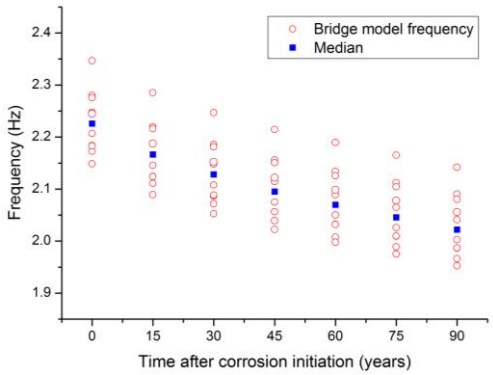

Figure 4. Time-dependent fundamental frequencies of the bridge models

4.2 Response analysis

In seismic design of RC bridges, the superstructure is required to remain in linear elastic range, while the columns are permitted to enter the nonlinear range to dissipate the

earthquake energy. Therefore, the seismic responses of the pier columns are critical in the life-cycle seismic performance evaluation of the RC bridges. In this paper, the maximum base moment and the drift ratio of the pier columns are taken as the life-cycle seismic performance index of the RC bridge under chloride induced corrosion. For each time step in each ground motion case, the mean values obtained from the 120 results (10 bridge models ×12 sets of ground motions) are presented and discussed in this study.

Figure 5 shows both the longitudinal and transverse mean maximum pier column base moments of the corrosion affected RC bridge in different time steps. As shown, the longitudinal maximum base moments are much larger than the transverse ones. This is because the first vibration mode of the analysed bridge is in the longitudinal direction. The maximum base moment in both directions decrease in the bridge's life-cycle, and the decreasing rate slows down with time. This is caused by the decrease of the corrosion current density in the bridge's service life as discussed above. Moreover, it can be noted that the ground motion spatial variations have a great effect on the life-cycle seismic responses of the corroded RC bridge. Completely neglecting ground motion spatial variation, i.e., the uniform ground motion case (Case 1), over predicts the seismic responses of the bridge as compared with those corresponding to the general case (Case 4). Considering only coherency loss effect (Case 3) results in the larger response, while considering only wave passage effect (Case 2) always underestimates the response. The ground motion case with heterogeneous site (Case 5) produces the maximum response. It can be also observed that the difference of mean response between the cases with different coherency loss (Cases 1 and 3; Cases 2 and 4) becomes smaller with time, and the cases with the same wave passage effect have rather similar base moments for the corroded bridge after being in service for 90 years since corrosion initiated. This is because that the chloride corrosion damage leads to bridge stiffness deterioration, and spatial ground motion wave passage effect is more pronounced to relatively flexible structures, while coherency loss effect is more prominent to relatively stiff structures, as reported by Hao and Duan (1996).

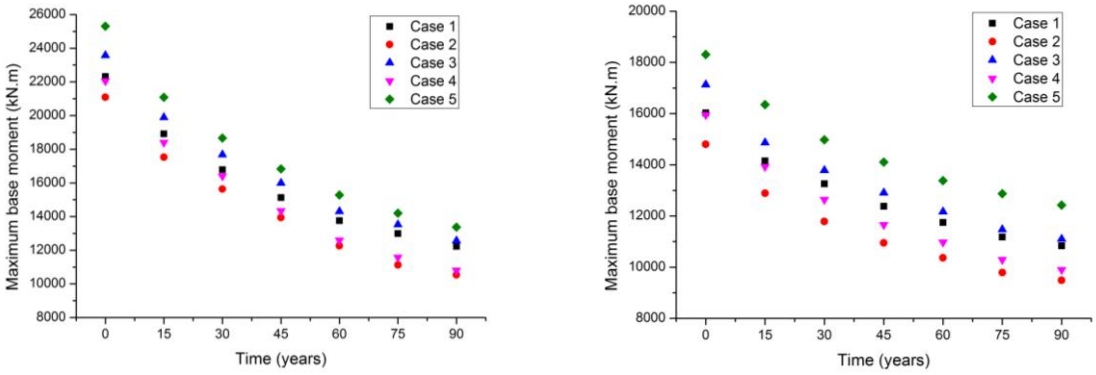

(a) Longitudinal direction (b) Transverse direction

Figure 5. Mean maximum base moments of the column in the (a) longitudinal and (b) transverse directions induced by different spatially varying ground motions

Figure 6 shows the mean maximum drift ratio of the column under different cases of spatial ground motions. The drift ratio of the column is defined by the SRSS of the longitudinal and transverse drift ratios. It can be observed that the mean maximum drift ratios increase in the bridge's life-cycle, and the increase trend slows down owning to the decrease of corrosion current density. Compared with the intact bridge (t_i=0), the mean maximum drift ratio increases by 28.3%, 20.2%, 20.8%, 16.6% and 22.5% for Case 1 to 5, respectively. Similar to the maximum moment, the difference between the maximum drift ratios under spatial ground motions with different coherency loss decreases with time, due to the same reason discussed above.

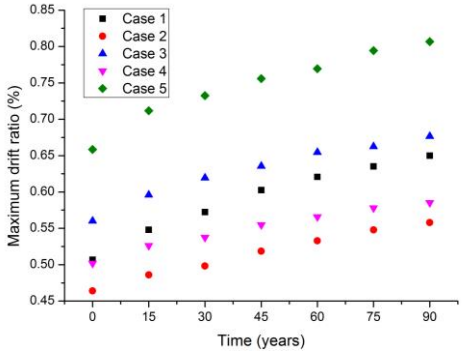

Figure 6. Mean maximum drift ratios of the column induced by different spatially varying ground motions

5. CONCLUSIONS

This paper investigates the life-cycle seismic responses of a chloride induced corrosion affected RC bridge subjected to spatially varying ground motions. The following conclusions can be drawn:

(1) Chloride induced corrosion may lead to a significant seismic performance degradation of RC bridges in their life-cycles, and it should not be neglected in the seismic response analysis.

(2) The seismic degradation trend in the bridge's life-cycle slows down with time owing to the decrease of chloride corrosion current density.

(3) Ground motion spatial variations have a great effect on the life-cycle seismic response of RC bridges. The spatial ground motion wave passage effect becomes more pronounced and the coherency loss effect becomes less prominent in the bridge's life-cycle, due to the stiffness deterioration of the RC bridge induced by continuous chloride corrosion.

ACKNOWLEDGEMENT

The authors acknowledge the partial financial support provided by Australain Reseach Council (ARC) linkage project LP110200906 for carrying out this research. The first author also acknowledges the financial support from China Scholarship Council for him to study in Australia.

REFERENCES

ASCE, (2013). Report card for America's infrastructure. <http://www.infrastructurereportcard.org/a/browser-options/downloads/2013-Report-Card.pdf>.

Aviram, A., Mackie, KR., Stojadinovic, B., (2008). Guidelines for nonlinear analysis of bridge structures in California, PEER Report, Pacific Earthquake Engineering Research Center, University of California Berkeley.

Alipour, A., Shafei, B., Shinozuka, M., (2010). Performance evaluation of deteriorating highway bridges located in high seismic areas, Journal of Bridge Engineering, Vol 16, No 5, pp 597-611.

Bi, K., Hao, H., (2012). Modelling and simulation of spatially varying earthquake ground motions at sites with varying conditions, Probabilistic Engineering Mechanics, Vol 29, pp 92-104.

Bi, K., Hao, H., (2013). Numerical simulation of pounding damage to bridge structures under spatially varying ground motions, Engineering Structures, Vol 46, pp 62-76.

Du, YG., Clark, LA., Chan, AHC., (2005). Residual capacity of corroded reinforcing bars. Magazine of Concrete Research, Vol 57, No 3, pp 135-147.

Ghosh, J., Padgett, JE., (2010). Aging considerations in the development of time-dependent seismic fragility curves, Journal of Structure Engineering, Vol 136, No 12, pp 1497-1511.

Hao, H., Oliveira, CS., Penzien, J., (1989). Multiple-station ground motion processing and simulation based on SMART-1 array data, Nuclear Engineering and Design, Vol 111, No 3, pp 293-310.

Hao, H., Duan, X., (1996). Multiple excitation effects on response of symmetric building, Engineering Structures, Vol 18, No 9, pp 732-740.

JTG/T B02-01, (2008). Guidelines for Seismic Design of Highway Bridges, Ministry of Communications of the People's Republic of China, 2008. (in Chinese)

Liu, T., Weyers, RW., (1998). Modeling the dynamic corrosion process in chloride contaminated concrete structures, Cement and Concrete Research, Vol 28, No 3, pp 365-379.

Pan, Y., Agrawal, AK., Ghosn, M., (2007). Seismic fragility of continuous steel highway bridges in New York State, Journal of Bridge Engineering, Vol 12, No 6, pp 689-699.

Simon, J., Bracci, JM., Gardoni, P., (2010). Seismic response and fragility of deteriorated reinforced concrete bridges, Journal of Structural Engineering, Vol 136, No 10, pp 1273-1281.

Stewart, MG., Rosowsky, DV., (1998). Time-dependent reliability of deteriorating reinforced concrete bridge decks, Structure Safaty, Vol 20, No 1, pp 91-109.

Vu, KAT., Stewart, MG., (2000). Structural reliability of concrete bridges including improved chloride-induced corrosion models, Structural Safety, Vol 22, No 4, pp 313-333.

Zanardo, G., Hao, H., Modena, C., (2002). Seismic response of multi-span simply supported bridges to spatially varying earthquake ground motion. Earthquake Engineering & Structural Dynamics, Vol 31, No 6, pp 1325-1345.